ELSEVIER

Journal of Photochemistry and Photobiology A: Chemistry 143 (2001) 23–29

Journal of Photochemistry and Photobiology A:Chemistry

www.elsevier.com/locate/jphotochem

2,4,6-Triphenylpyrylium ion-mediated photooxidation of *N*,*N*-dibenzylhydroxylamine and its derivatives

Yukinori Iijima [a], Shuko Obara [a], Yasuhiro Ohba [a], Kanji Kubo [b], Tadamitsu Sakurai [a,*]

[a] *Department of Applied Chemistry, Faculty of Engineering, Kanagawa University, Kanagawa-ku, Yokohama 221-8686, Japan*
[b] *Institute of Advanced Material Study, Kyushu University, Kasuga-Koen, Kasuga 816-0811, Japan*

Received 1 February 2001; received in revised form 2 April 2001; accepted 2 May 2001

Abstract

The irradiation of an O_2-purged MeCN solution of *N*,*N*-dibenzylhydroxylamine and its derivatives (**1**) in the presence of 2,4,6-triphenylpyrylium tetrafluoroborate (TPT) with 366 nm light was found to give the corresponding *N*-benzylidenebenzylamine *N*-oxide derivative and 2,4,6-triphenyl-3,4-epoxypyran. Solvent effects on the fluorescence quenching of TPT by **1** and the quantum yield for the disappearance of TPT (Φ_{TPT}) strongly suggested that electron transfer to both singlet and triplet TPT occurs, particularly on the low concentration sides of **1**, affording the hydroxylamine radical cation ($\mathbf{1}^{\bullet+}$) and the TPT-derived pyranyl radical ($\mathrm{TP}^{\bullet}$). Furthermore, substituent effects on the limiting quantum yield ($\Phi_{\mathrm{TPT,lim}}$) showed that the increased stability of $\mathbf{1}^{\bullet+}$ lowers the return electron-transfer rate to enhance the relative reactivity of $\mathrm{TP}^{\bullet}$ toward O_2, that is, to increase $\Phi_{\mathrm{TPT,lim}}$. On the other hand, analysis of heavy atom effects on the TPT emission intensity and the photooxidation efficiency led us to conclude that the presence of 1,2-dibromoethane accelerates intersystem crossing to the excited triplet-state TPT through the enhanced spin–orbit coupling resulting in an increase in Φ_{TPT}. The observed heavy atom effects on Φ_{TPT} were explained in terms of the increased contribution of a triplet $\mathbf{1}^{\bullet+}$–$\mathrm{TP}^{\bullet}$ pair intermediate in which spin-forbidden reverse electron transfer is responsible for a great enhancement in the reactivity of $\mathrm{TP}^{\bullet}$ toward O_2.

Keywords: *N*,*N*-dibenzylhydroxylamines; 2,4,6-Triphenylpyrylium salt; Photooxidation; Substituent effect; Heavy atom effect

1. Introduction

Electron transfer photooxygenation reactions of organic compounds have been extensively studied during the past decade from both synthetic and mechanistic points of view [1,2]. It has been well confirmed that depending on solvent polarity as well as on the structure of an unsaturated substrate, singlet oxygen or superoxide ion or both can be involved as a crucial oxidant in cyanoaromatics-sensitized photooxygenations [3–11]. In addition to these cyanoaromatics, 2,4,6-triphenylpyrylium tetrafluoroborate (TPT) is also very frequently used as an electron-transfer photosensitizer owing to a unique property that it produces neither singlet oxygen nor superoxide ion [12–21]. This property of TPT made it possible to investigate directly the interaction between molecular oxygen and substrate radical cations formed by electron transfer. However, there are only a few studies directed toward the elucidation of the behavior of 2,4,6-triphenylpyranyl radical in the presence of molecular oxygen [22,23].

In previous studies [24–27] we demonstrated that substituted *N*,*N*-dibenzylhydroxylamines (**1**) undergo 9,10-dicyanoanthracene (DCA)-sensitized photooxidation giving quantitatively the corresponding *N*-benzylidenebenzylamine *N*-oxide derivative (**2**) and hydrogen peroxide. Thermodynamic and kinetic analyses of these oxidation reactions showed that superoxide ion is involved as the major oxidant in the process and then the oxidation efficiency is determined by the relative rate of back electron transfer within the geminate radical ion pair [27]. Since little is known about the reactivity of the hydroxylamine-derived radical cation toward O_2, the TPT-sensitized photooxidation of **1** may be a good system for exploring the behavior of the hydroxylamine radical cation and the TPT-derived pyranyl radical in an atmosphere of O_2. On the other hand, both the excited singlet and triplet states of TPT are known to participate in the electron-transfer process from organic substrates [14,23,28,29]. It is, thus, important to estimate the extent to which photoinduced electron transfer takes place from the excited singlet-state of TPT. Taking into account the background described above, we chose the hydroxylamines **1a–c** as substrates and investigated substituent and heavy atom effects on the quantum yield for the photooxidation

---

* Corresponding author. Tel.: +81-45-481-5661; fax: +81-45-491-7915.
E-mail address: sakurt01@kanagawa-u.ac.jp (T. Sakurai).

1010-6030/01/$ – see front matter
PII: S1010-6030(01)00469-5

reaction of **1b** in O_2-saturated MeCN containing TPT, in order to elucidate the behavior of the hydroxylamine radical cation as well as the pyranyl radical in the presence of molecular oxygen.

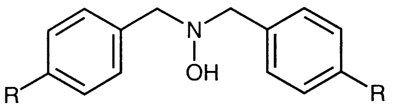

1

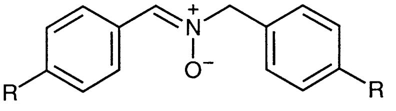

2

R= Me (**1a**), H (**1b**), CF_3 (**1c**)

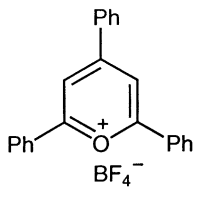

TPT

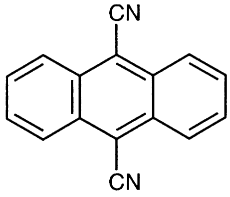

DCA

2. Results and discussion

2.1. Product analysis and fluorescence quenching of TPT

In Fig. 1 are shown UV absorption spectral changes caused by the 366 nm irradiation of an O_2-purged MeCN solution of **1b** (5.0×10^{-4} mol dm^{-3}) containing TPT (5.0×10^{-5} mol dm^{-3}) at room temperature. In contrast with the DCA-sensitized photooxidation where the absorption of this sensitizer remains unchanged during irradiation [24–27], the TPT absorption at 354 nm decreased with the appearance of the 298 nm absorption originating from the oxidation product **2b**. An analysis of Fig. 1 reveals that the amount of TPT disappeared is in fair agreement with that of **2b** formed. Similar absorption spectral changes were observed also for the starting **1a** and **1c**. In order to isolate **2b** and TPT-derived product(s), an O_2-saturated MeCN solution of **1b** (1.3×10^{-2} mol dm^{-3}) was irradiated in the presence of TPT (2.6×10^{-3} mol dm^{-3}) with light of wavelengths longer than 340 nm. The product mixture obtained was subjected to column and/or preparative thin-layer chromatography over silica gel, which allowed us to isolate **2b** and 2,4,6-triphenyl-3,4-epoxypyran (**3**) (Scheme 1). The yields of **2b** and **3** based on consumed TPT (32%) were 64 and 56%, respectively. In addition, we detected small amounts of benzaldehyde and **3**-derived decomposition products, showing that both **2b** and **3** undergo breakdown to these byproducts during workup. The successful isolation of **3** demonstrates that 2,4,6-triphenyl-4-hydroperoxypyran serves as the precursor of this epoxide. On the other hand, iodometry of the solution irradiated gave no indication of the formation of hydrogen peroxide, being inconsistent with either a singlet oxygen or a superoxide ion mechanism.

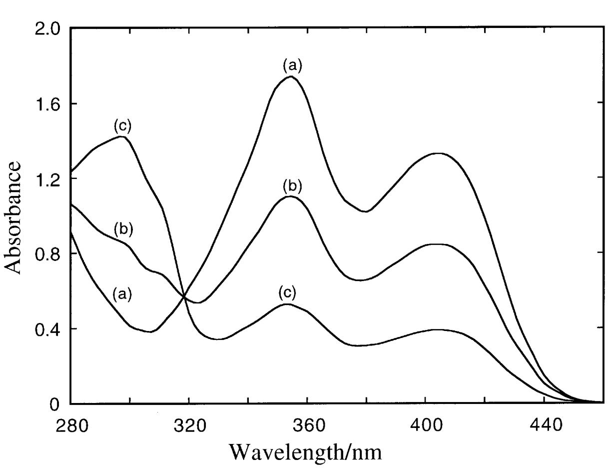

Fig. 1. UV absorption spectral changes of TPT (5.0×10^{-5} mol dm^{-3}) and **1b** (5.0×10^{-4} mol dm^{-3}) during irradiation in O_2-purged MeCN at room temperature. Irradiation wavelength = 366 nm. Irradiation time (min): (a) 0; (b) 30; (c) 60.

As typically shown in Fig. 2, the fluorescence of TPT was efficiently quenched by **1b** according to the Stern–Volmer equation (Eq. (1)) in N_2-saturated MeCN at room temperature

$$\frac{I_0}{I} = 1 + k_{\mathrm{et}}\tau_{\mathrm{S}}\,[\mathbf{1b}] \qquad (1)$$

where I and I_0 are the fluorescence intensities of TPT with and without **1b**, k_{et} the rate constant for the fluorescence quenching process and τ_{S} the fluorescence lifetime of TPT

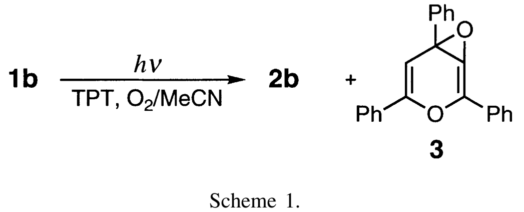

Scheme 1.

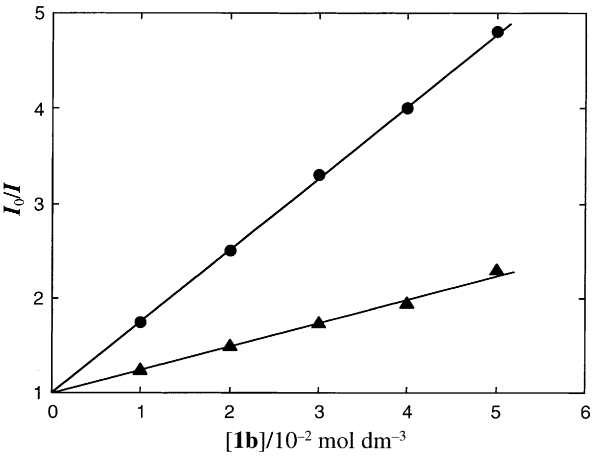

Fig. 2. Stern–Volmer plots for the fluorescence quenching of TPT (5.0×10^{-5} mol dm^{-3}) by **1b** in N_2-saturated MeCN (●) and 1,2-dichloroethane (▲) at room temperature. Excitation wavelength = 366 nm.

in the absence of **1b**. From the slope of the linear plot and the τ_S value of 4.4 ns, the rate constant k_{et} was estimated to be 1.7×10^{10} dm^3 mol^{-1} s^{-1}, being consistent with the occurrence of the emission quenching at the diffusion-limited rate. The simplified Weller equation (Eq. (2)) allowed us to calculate the free energy change (ΔG_{et}) for electron transfer from **1a–c** to singlet TPT (the sign and magnitude of which provides a good criterion for the involvement of electron transfer) [30,31] and the ΔG_{et} and k_{et} values were collected in Table 1 along with related parameters.

$$\Delta G_{et}\,(\mathrm{kJ\,mol^{-1}}) = 96.5(E_{ox} - E_{red}) - E_S \qquad (2)$$

where E_{ox}, E_{red} and E_S refer to the oxidation potential of **1**, the reduction potential of TPT (−0.38 V versus SCE in MeCN [32]) and the first singlet excitation energy of TPT (270 kJ mol^{-1} in MeCN [33]), respectively. Because singlet–singlet energy transfer from singlet TPT to **1** ($E_S \approx 350$ kJ mol^{-1} [25]) is highly endothermic, the large negative value of ΔG_{et} (−169 to −137 kJ mol^{-1}) presents strong evidence for the exclusive electron transfer fluorescence quenching in MeCN. The finding that the rate constant k_{et} has a propensity to increase with a decrease in the oxidation potential of **1** also substantiates a fluorescence quenching mechanism via electron transfer. Thus, the results of the product analysis and the TPT fluorescence quenching lead us to propose Scheme 2 in which 2,4,6-triphenylpyran-4-peroxyl radical (formed by the reaction of the pyranyl radical with O_2) is a key intermediate in the oxidation process. On the other hand, the fluorescence of TPT was less efficiently quenched in 1,2-dichloroethane than in MeCN (Fig. 2). The slope of the linear Stern–Volmer plots and the TPT fluorescence lifetime of 3.2 ns in 1,2-dichloroethane allowed us to estimate the k_{et} values listed in Table 1. Though we have not a thermodynamic criterion for the involvement of electron transfer in this less polar solvent, the finding that the k_{et} increases with increasing electron-donating ability of the substituents of **1a–c** is consistent with the occurrence of electron transfer fluorescence quenching.

$$\mathrm{TPT} \xrightarrow{h\nu} {}^1\mathrm{TPT}$$
$${}^1\mathrm{TPT} \xrightarrow{1/\tau_S} \mathrm{TPT}$$
$${}^1\mathrm{TPT} + \mathbf{1} \xrightarrow{k_{et}} \mathrm{TP}^{\bullet}\,\mathrm{BF_4}^- + \mathbf{1}^{+\bullet}$$
$$\mathrm{TP}^{\bullet}\,\mathrm{BF_4}^- + \mathbf{1}^{+\bullet} \xrightarrow{k_{-et}} \mathrm{TPT} + \mathbf{1}$$
$$\mathrm{TP}^{\bullet}\,\mathrm{BF_4}^- + \mathbf{1}^{+\bullet} + \mathrm{O_2} \xrightarrow{k_r} \mathrm{TP{-}OOH} + \mathbf{2} + \mathrm{HBF_4}$$
$$\mathrm{TP{-}OOH} \xrightarrow{k_r'} \mathbf{3} + \mathrm{H_2O}$$

Scheme 2.

2.2. *Quantum yields for the photooxidation reactions*

All of the photooxidation products do not exhibit any absorption at 404 nm where TPT gives its strong absorption (molar absorption coefficient, $\varepsilon = 2.6 \times 10^4$ dm^3 mol^{-1} cm^{-1}). However, the relatively weak absorption of the epoxide **3** is observed at 298 nm ($\varepsilon = 3.2 \times 10^3$ dm^3 mol^{-1} cm^{-1}) so that we are not able to accurately determine the concentration of the *N*-oxide **2** produced. By applying the steady-state approximation to Scheme 2, we obtain Eq. (3) which relates the quantum yield for the disappearance of TPT (Φ_{TPT}) to the concentration of the

Table 1
Stern–Volmer constants, fluorescence quenching rate constants, oxidation potentials of **1a–c** and free energy changes associated with electron transfer from **1** to the excited singlet-state TPT at room temperature

Compound	Solvent	$k_{et}\tau_S$ (M^{-1})	k_{et} (M^{-1} s^{-1})	E_{ox} (V)[a]	ΔG_{et} (kJ mol^{-1})
1a	MeCN	82	1.9×10^{10}	0.67	−169
	CH_2ClCH_2Cl	28	0.86×10^{10}	–	–
1b	MeCN	76	1.7×10^{10}	0.76	−160
	CH_2ClCH_2Cl	24	0.75×10^{10}	–	–
1c	MeCN	55	1.2×10^{10}	1.00	−137
	CH_2ClCH_2Cl	13	0.40×10^{10}	–	–

[a] Values vs. SCE [27]; 1 M = 1 mol dm^{-3}.

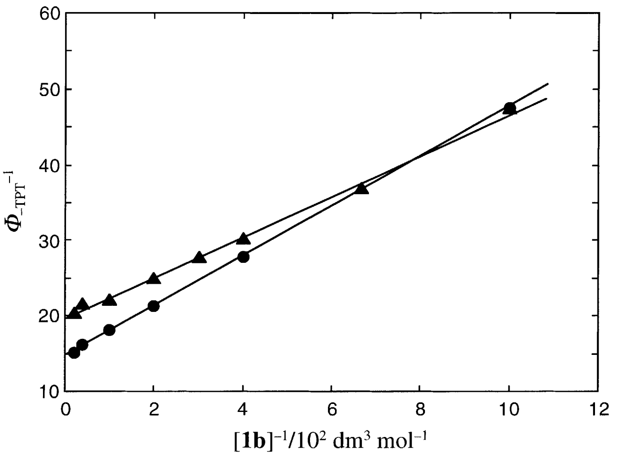

Fig. 3. Stern–Volmer plots of $(\Phi_{\rm TPT})^{-1}$ vs. $[\mathbf{1b}]^{-1}$ for the photooxidation of **1b** in the presence of TPT (5.0×10^{-5} mol dm^{-3}) in O_2-purged MeCN (●) and 1,2-dichloroethane (▲) at room temperature. Irradiation wavelength = 366 nm.

starting hydroxylamine **1**

$$\frac{1}{\Phi_{\rm TPT}}=\left(1+\frac{k_{-\rm et}}{k_{\rm r}[{\rm O_2}]}\right)\left(1+\frac{1}{k_{\rm et}\tau_{\rm S}\,[\mathbf{1}]}\right) \tag{3}$$

As shown in Fig. 3, the observation of the linear Stern–Volmer plots of $1/\Phi_{\rm TPT}$ against the reciprocal concentration of **1** ($1/[\mathbf{1}]$) is consistent with Scheme 2 proposed for the TPT-mediated photooxidation reaction of **1**. From the intercept and the ratio of the intercept to slope of these linear plots, we can estimate the limiting quantum yields for the disappearance of TPT ($\Phi_{\rm TPT,lim}=k_{\rm r}[{\rm O_2}]/(k_{\rm r}[{\rm O_2}]+k_{-\rm et})$) and the $k_{\rm et}\tau_{\rm S}$ values, respectively. Because the $k_{\rm et}\tau_{\rm S}$ value can be determined independently through an analysis of the fluorescence quenching of TPT by **1**, it is possible to compare this quenching constant obtained by two different procedures. In Table 2 are collected the $\Phi_{\rm TPT,lim}$, $k_{\rm r}[{\rm O_2}]/k_{-\rm et}$ and $k_{\rm et}\tau_{\rm S}$ values determined in MeCN and 1,2-dichloroethane. Even though the indirect and yet different procedures for the estimation of $k_{\rm et}\tau_{\rm S}$ necessarily lead to a large error, the $k_{\rm et}\tau_{\rm S}$ value determined from the linear plot of $1/\Phi_{\rm TPT}$ versus $1/[\mathbf{1}]$ (particularly in 1,2-dichloroethane) is much larger than that obtained from the TPT fluorescence quenching. Since TPT has a high quantum yield for intersystem crossing ($\Phi_{\rm isc}=0.48$ [12] and 0.42 [23]), this finding suggests some contribution of electron transfer to the excited triplet-state TPT on the low concentration sides of **1**. Therefore, we are led to propose that the *N*-oxide **2** and the epoxide **3** can be formed via electron transfer from **1** to both the excited singlet- and triplet-state TPT.

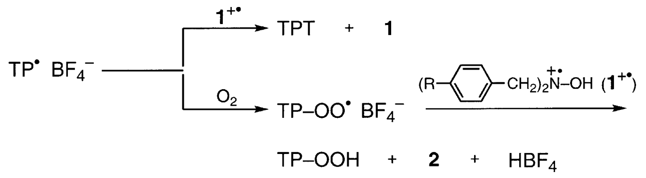

Scheme 3.

The increased concentration of **1** should reduce the contribution of the triplet-state electron transfer process relative to the singlet-state process, and hence the use of $\Phi_{\rm TPT,lim}$ makes it possible to discuss substituent and solvent effects on the behavior of the singlet TPT-derived pyranyl radical (TP$^\bullet$) and hydroxylamine radical cation ($\mathbf{1}^{\bullet+}$) without a consideration of these effects on the quenching rate constant and the extent of the contribution of electron transfer in the excited triplet-state. Because reverse electron transfer between $\mathbf{1}^{\bullet+}$ and TP$^\bullet$ (regenerating the starting **1** and TPT) competes with the reaction of O_2 with TP$^\bullet$ forming the pyranperoxyl radical (Scheme 3), an inspection of the relation, $1/\Phi_{\rm TPT,lim}=1+k_{-\rm et}/(k_{\rm r}[{\rm O_2}])$, reveals that the relative rate of back electron transfer to attack of O_2 on TP$^\bullet$ determines the oxidation efficiency of **1**. As is obvious from Table 2, the rate of back electron transfer is much greater than the rate for formation of the pyranperoxyl radical (TP–OO$^\bullet$), irrespective of solvent polarity and substituents, resulting in a drop in the reactivity of the radical cation intermediate $\mathbf{1}^{\bullet+}$. Based on the equation: $\Delta G_{-\rm et}$ (kJ mol^{-1}) $=-96.5(E_{\rm ox}-E_{\rm red})$, the free energy change for the reverse electron transfer process ($\Delta G_{-\rm et}$) was evaluated to be −101 (**1a**), −110 (**1b**) and −133 (**1c**) kJ mol^{-1}. Accordingly, in addition to the large exothermicity for electron transfer from TP$^\bullet$ to $\mathbf{1}^{\bullet+}$, steric hindrance of the phenyl group at the 4-position in TP$^\bullet$ should also be responsible for a lowering of the reactivity of TP$^\bullet$ toward O_2.

Despite the low photooxidation efficiency of **1a–c**, there is a clear-cut tendency for the relative rate $k_{\rm r}[{\rm O_2}]/k_{-\rm et}$ to

Table 2
Stern–Volmer constants, limiting quantum yields and related parameters for the TPT-mediated photooxidation of **1a–c** at room temperature

Compound	Solvent	$k_{\rm et}\tau_{\rm S}$ (M^{-1})[a]	$k_{\rm et}\tau_{\rm S}$ (M^{-1})[b]	$\Phi_{\rm TPT,lim}$	$k_{\rm r}[{\rm O_2}]/k_{-\rm et}$
1a	MeCN	82	270	0.108 ± 0.006	0.11
	CH_2ClCH_2Cl	28	730	0.061 ± 0.002	0.063
1b	MeCN	76	440	0.070 ± 0.002	0.077
	CH_2ClCH_2Cl	24	740	0.050 ± 0.002	0.053
1c	MeCN	55	390	0.032 ± 0.002	0.032
	CH_2ClCH_2Cl	13	330	0.016 ± 0.001	0.016

[a] Determined from the fluorescence quenching of TPT by **1a–c**.
[b] Determined from the dependence of $\Phi_{\rm TPT}$ on [**1**]; 1 M = 1 mol dm^{-3}.

increase as the electron-donating ability of the substituent R is increased in any solvent (Table 2). As already described above, the rate for the reaction between TP$^\bullet$ and O_2 governs the magnitude of $k_r[O_2]$ and then is considered to undergo no substituent effects. Thus, an analysis of the dependence of $k_r[O_2]/k_{-et}$ on ΔG_{et} leads us to conclude that the back electron transfer takes place in the Marcus 'normal region' [34]. In other words, the increased stability of $\mathbf{1}^{\bullet +}$ lowers the back electron-transfer rate to enhance the relative reactivity of TP$^\bullet$ toward O_2, that is, to increase the limiting quantum yield for the photooxidation of **1** in the presence of TPT. On the other hand, any starting hydroxylamine gives a smaller $k_r[O_2]/k_{-et}$ value in 1,2-dichloroethane than in MeCN. Lower reactivities of $\mathbf{1}^{\bullet +}$ and TP$^\bullet$ obtained by electron transfer in the former solvent may be in part due to the decreased stability of $\mathbf{1}^{\bullet +}$ in this less polar solvent, which contributes to accelerating the back electron transfer reaction.

2.3. Heavy-atom effects on the quantum yield and the TPT phosphorescence

It has been found that TPT gives characteristic fluorescence and phosphorescence emissions and undergoes an external heavy-atom effect which increases the rate for singlet–triplet interconversion through spin–orbit coupling [12,28]. Since the enhanced formation of triplet TPT by the heavy-atom effect is accompanied by the increased quenching of singlet TPT, we may expect a great contribution of the photooxidation reaction initiated by electron transfer to triplet TPT. For the purpose of obtaining evidence for the participation of triplet TPT, we chose **1b** as a starting hydroxylamine and examined the heavy-atom effect of added 1,2-dibromoethane (DBE) on the TPT emission as well as on the reaction quantum yield (Φ_{TPT}).

The Stern–Volmer plots given in Fig. 4 demonstrate that the TPT fluorescence is significantly quenched in the presence of DBE and 1,2-dichloroethane exerts its heavy atom effect to only a small extent. The small but perceivable heavy-atom effect of the latter additive substantiates the idea that the triplet-state electron transfer process contributes to a larger extent in 1,2-dichloroethane than in MeCN containing low concentrations of **1** to render the slope of the linear plot of $1/\Phi_{TPT}$ versus $1/[\mathbf{1}]$ smaller in the former solvent, as observed. If DBE could accelerate intersystem crossing to the excited triplet state through the enhanced spin–orbit coupling, the fluorescence quenching should be accompanied by an increase in the phosphorescence intensity (I_P) of TPT [35]. It can be seen from Fig. 5 that the phosphorescence intensity ratio at 520 nm increases almost linearly with increasing the concentration of added DBE even at 77 K [$I_P([\text{DBE}] = 17.0\,\text{vol.\%})/I_P([\text{DBE}] = 0) = 4.1$]. Thus, we are allowed to expect a large contribution of the photooxidation reaction proceeding through triplet TPT when the reaction is conducted in the presence of DBE.

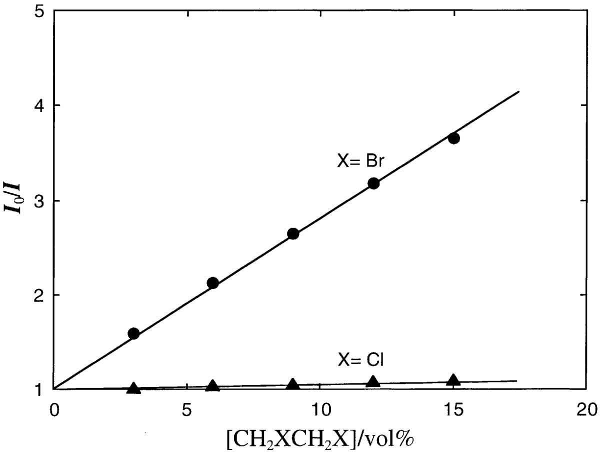

Fig. 4. Stern–Volmer plots for the fluorescence quenching of TPT (5.0×10^{-5} mol dm^{-3}) by DBE (●) and 1,2-dichloroethane (▲) in N_2-saturated MeCN at room temperature. Excitation wavelength = 366 nm.

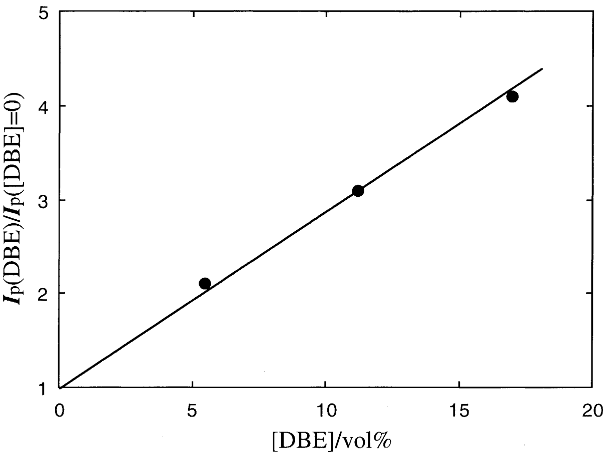

Fig. 5. Phosphorescence intensity ratio of TPT (5.0×10^{-5} mol dm^{-3}) as a function of the DBE concentration in butyronitrile at 77 K. I_p(DBE) and $I_P([\text{DBE}] = 0)$ refer to the phosphorescence intensities of TPT with and without DBE, respectively. Excitation wavelength = 366 nm.

In Table 3 are shown quantum yields for the reaction of **1b** (Φ_{TPT}) determined in O_2-purged MeCN containing TPT and DBE under the same irradiation conditions. Evidently, the increased concentration of DBE results in a significant increase in Φ_{TPT} at any concentrations of **1b**, confirming that the triplet TPT-mediated oxidation of **1** gives **2** and **3** in much higher quantum yields, as compared to the singlet TPT-mediated reaction. As already discussed, the occurrence of return electron transfer from TP$^\bullet$ to $\mathbf{1}^{\bullet +}$ in preference to the reaction with O_2 must be responsible for the low oxidation efficiency of singlet TPT. The finding that electron transfer to triplet TPT having the excitation energy of 222 kJ mol^{-1} [36] is also highly exothermic process ($\Delta G_{et} = -121$ to -89 kJ mol^{-1}) indicates this electron transfer to take place efficiently forming TP$^\bullet$ to $\mathbf{1}^{\bullet +}$. What is the factor that renders the triplet TPT-derived pyranyl radical and hydroxylamine radical cation more reactive? Taking into account that there is an energy barrier

Table 3
Quantum yields for the disappearance of TPT (Φ_{TPT}) for the photooxidation of **1b** in an O_2-purged MeCN containing TPT and DBE at room temperature

[DBE] (vol.%)	[**1b**] (10^{-3} mol dm^{-3})					
	1.0	2.5	5.0	10	25	50
0	0.021 ± 0.001	0.036 ± 0.002	0.047 ± 0.002	0.055 ± 0.003	0.062 ± 0.004	0.066 ± 0.004
5.5	0.058 ± 0.006	0.087 ± 0.008	0.113 ± 0.007	0.136 ± 0.008	0.143 ± 0.009	0.141 ± 0.011
17.0	0.079 ± 0.004	0.114 ± 0.006	0.155 ± 0.008	0.185 ± 0.016	0.206 ± 0.020	0.203 ± 0.021

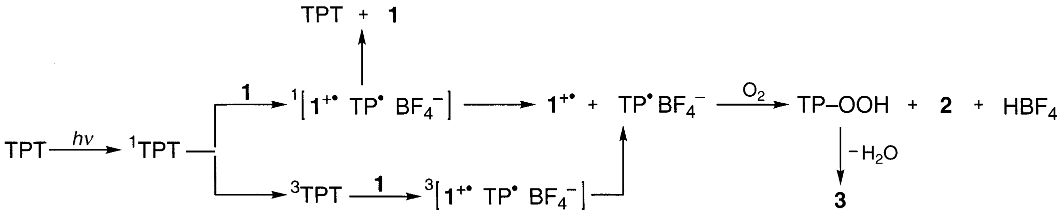

Scheme 4.

to a change in spin multiplicity, we propose the triplet hydroxylamine radical cation and pyranyl radical pair $^3[\mathbf{1}^{\bullet+}\ \mathrm{TP}^{\bullet}\ \mathrm{BF_4}^-]$ initially formed by electron transfer from **1** to triplet TPT. Because spin inversion to the singlet radical cation–radical pair $^1[\mathbf{1}^{\bullet+}\ \mathrm{TP}^{\bullet}\ \mathrm{BF_4}^-]$ must precede return electron transfer to give the ground singlet-state **1** and TPT, the presence of an energy barrier to return electron transfer results in preferential diffusive separation of $\mathbf{1}^{\bullet+}$ and $\mathrm{TP}^{\bullet}$ from the spin-correlated radical cation–radical pair [37] and, hence, in a much more enhancement of the reactivity of $\mathrm{TP}^{\bullet}$ toward O_2 in $^3[\mathbf{1}^{\bullet+}\ \mathrm{TP}^{\bullet}\ \mathrm{BF_4}^-]$ than in $^1[\mathbf{1}^{\bullet+}\ \mathrm{TP}^{\bullet}\ \mathrm{BF_4}^-]$. It is, therefore, reasonable to interpret the observed heavy-atom effects on Φ_{TPT} in terms of the increased contribution of the former radical cation–radical pair mechanism. This interpretation is also supported by the recent finding that iodobenzene in MeCN quenches singlet TPT more rapidly than triplet TPT by three orders of magnitude [28]. Moreover, it is very likely that (even in the absence of DBE) the TPT-mediated photooxidation of low concentrations of **1** takes place by both singlet and triplet radical cation–radical pair mechanisms, as manifested in Scheme 4.

3. Experimental details

3.1. Measurements

Ultraviolet (UV) absorption and fluorescence spectra were recorded on a Shimadzu Model UV-2200 spectrophotometer and a Shimadzu Model RF-5000 spectrofluorimeter, respectively. Fluorescence lifetimes were measured under N_2 at room temperature with a time-correlated single-photon counting apparatus (Horiba NAES-700; excitation wavelength = 366 nm; cut-off wavelength = 410 nm). Phosphorescence spectra at 77 K were measured on a Hitachi Model F-4500 spectrofluorimeter equipped with attachments for measuring low temperature phosphorescence. Nuclear magnetic resonance (NMR) spectra were recorded on a JEOL Model JNM-A500 spectrometer. Infrared (IR) spectra were taken with a Hitachi Model 270-30 infrared spectrometer. Elemental analyses were performed on a Perkin-Elmer PE2400 series II CHNS/O analyzer.

A potassium tris(oxalato)ferrate(III) actinometer was employed to determine the quantum yields for the disappearance of TPT at its low conversion (<20%) [38]. A 450 W high pressure Hg lamp was used as the light source from which 366 nm light was selected with Corning 0-52, Corning 7-60 and Toshiba IRA-25S glass filters. The molar absorption coefficients of TPT at 404 nm in MeCN (2.6×10^4 dm^3 mol^{-1} cm^{-1}) and at 416 nm in 1,2-dichloroethane (2.5×10^4 dm^3 mol^{-1} cm^{-1}) were utilized to quantify the disappearance of TPT. Quantum yields for the photooxidation reaction in DBE-containing MeCN were measured similarly. All of the quantum yields are an average of more than five determinations.

3.2. Materials and solvents

N,*N*-bis(*p*-substituted benzyl)hydroxylamines (**1a**–**c**) were prepared from the reactions of *p*-substituted benzyl chlorides with hydroxylamine in a refluxing aqueous ethanol solution, according to the method of Jones and Sneed [39]. Crude products obtained were purified by repeated recrystallization from EtOAc–hexane. Physical and spectroscopic properties of **1a**–**c** were compatible with those of previously prepared and purified samples [25]. *N*-benzylidenebenzylamine *N*-oxide (**2b**) was the same as that previously employed [25]. TPT was recrystallized twice from EtOH containing small amounts of MeCN.

1,2-Dichloroethane was of spectroscopic grade and was used as received. Purification of MeCN, butyronitrile and DBE were accomplished by the standard methods [40].

3.3. Product analysis

A solution of **1b** ($1.3 \times 10^{-2}\,\mathrm{mol\,dm^{-3}}$) and TPT ($2.6 \times 10^{-3}\,\mathrm{mol\,dm^{-3}}$) in MeCN (500 ml), placed in a Pyrex vessel, was irradiated for 150 min under O_2 at room temperature with light of wavelengths longer than 340 nm, which was selected with an aqueous solution filter of sodium metavanadate ($1.0 \times 10^{-2}\,\mathrm{mol\,dm^{-3}}$) dissolved in $0.1\,\mathrm{mol\,dm^{-3}}$ sodium hydroxide, from a 400 W high pressure Hg lamp [41]. After 150 min irradiation, an appropriate amount of the solution (5 ml) being irradiated was pipetted off and subjected to iodometry. The remaining solution was concentrated to dryness under reduced pressure and the resulting residue was subjected to column (230 mesh, Merck) and/or preparative thin layer (Merck) chromatography over silica gel eluting with EtOAc–hexane. Physical and spectroscopic properties of the isolated products **2b** and 2,4,6-triphenyl-3,4-epoxypyran (**3**) are as follows.

2b: Mp 81.5–83.5°C. IR (KBr) ν: 3064, 1587, 1458, 1152 $\mathrm{cm^{-1}}$. ^{1}H NMR (500 MHz; $CDCl_3$) δ: 5.04 (2H, s), 7.38–7.47 (9H, m), 8.19–8.21 (2H, m). These physical and spectroscopic properties were in agreement with those of previously prepared authentic sample [25].

3: Mp 116.0–117.0°C. IR (KBr) ν: 3046, 1602, 1266, 891 $\mathrm{cm^{-1}}$. ^{1}H NMR (500 MHz, $CDCl_3$) δ: 6.99 (1H, s), 7.29–7.47 (8H, m), 7.53 (1H, dddd, $J = 7.3, 7.3, 1.7, 1.7$ Hz), 7.61 (2H, dd, $J = 8.6, 1.6$ Hz), 7.79 (2H, dd, $J = 7.9, 1.2$ Hz), 7.95 (2H, dd, $J = 8.4, 1.5$ Hz). ^{13}C NMR ($CDCl_3$) δ: 77.2, 109.8, 125.0, 128.1, 128.2, 128.4, 129.0, 129.2, 129.29, 129.32, 129.8, 132.2, 137.7, 138.1. MS *m/z* (relative intensity): 324 (M^+, 100%). Analysis: calculated for $C_{23}H_{16}O_2$: C, 85.16%; H, 4.97%; found: C, 84.83%; H, 5.12%.

References

[1] P.S. Mariano, J.L. Stavinoha, in: W.M. Horspool (Ed.), Synthetic Organic Photochemistry, Plenum Press, New York, 1984, p. 145.
[2] G.J. Kavarnos, N.J. Turro, Chem. Rev. 86 (1986) 419.
[3] J. Eriksen, C.S. Foote, T.L. Parker, J. Am. Chem. Soc. 99 (1977) 6455.
[4] A.P. Schaap, K.A. Zaklika, B. Kaskar, L.W.-M. Fung, J. Am. Chem. Soc. 102 (1980) 389.
[5] J. Eriksen, C.S. Foote, J. Am. Chem. Soc. 102 (1980) 6083.
[6] D.S. Steichen, C.S. Foote, J. Am. Chem. Soc. 103 (1981) 1855.
[7] J. Santamaria, Tetrahedron Lett. 22 (1981) 4511.
[8] Y. Araki, D.C. Dobrowolski, T.E. Goyne, D.C. Hanson, Z.Q. Jiang, K.J. Lee, C.S. Foote, J. Am. Chem. Soc. 106 (1984) 4570.
[9] K. Gollnick, A. Schnatterer, Photochem. Photobiol. 43 (1986) 365.
[10] F.D. Lewis, A.M. Bedell, R.E. Dykstra, J.E. Elbert, I.R. Gould, S. Farid, J. Am. Chem. Soc. 112 (1990) 8055.
[11] S.K. Silverman, C.S. Foote, J. Am. Chem. Soc. 113 (1991) 7672.
[12] M.A. Miranda, H. García, Chem. Rev. 94 (1994) 1063.
[13] H. García, M.A. Miranda, F. Mojarrad, M.-J. Sabater, Tetrahedron 50 (1994) 8773.
[14] N. Manoj, K.R. Gopidas, J. Photochem. Photobiol. A: Chem. 85 (1995) 53.
[15] P. Gaviña, N.L. Lavernia, R. Mestres, M.A. Miranda, Tetrahedron 52 (1996) 4911.
[16] Y. Chen, S.-K. Wu, J. Photochem. Photobiol. A: Chem. 102 (1997) 203.
[17] K.-D. Warzecha, M. Demuth, H. Görner, J. Chem. Soc., Faraday Trans. 93 (1997) 1523.
[18] S.S. Jayanthi, P. Ramamurthy, J. Phys. Chem. A 101 (1997) 2016.
[19] J. Delgado, A. Espinós, M.C. Jiménez, M.A. Miranda, R. Tormos, Tetrahedron 53 (1997) 681.
[20] M. Sridhar, B.A. Kumar, Chem. Lett. (1998) 461.
[21] F. Galindo, M.A. Miranda, J. Photochem. Photobiol. A: Chem. 113 (1998) 155.
[22] R. Akaba, S. Aihara, H. Sakuragi, K. Tokumaru, J. Chem. Soc., Chem. Commun. (1987) 1262.
[23] R. Akaba, H. Sakuragi, K. Tokumaru, J. Chem. Soc., Perkin Trans. 2 (1991) 291.
[24] T. Sakurai, Y. Uematsu, O. Tanaka, H. Inoue, J. Chem. Soc., Chem. Commun. (1991) 1425.
[25] T. Sakurai, Y. Uematsu, O. Tanaka, H. Inoue, J. Chem. Soc., Perkin Trans. 2 (1992) 2163.
[26] T. Sakurai, M. Yokono, K. Komiya, Y. Masuda, H. Inoue, J. Chem. Soc., Chem. Commun. (1993) 1689.
[27] T. Sakurai, M. Yokono, K. Komiya, Y. Masuda, H. Inoue, J. Chem. Soc., Perkin Trans. 2 (1994) 2515.
[28] P. Ramamurthy, S. Parret, F. Morlet-Savary, J.P. Fouassier, J. Photochem. Photobiol. A: Chem. 83 (1994) 205.
[29] S.S. Jayanthi, P. Ramamurthy, J. Phys. Chem. A 102 (1998) 511.
[30] D. Rehm, A. Weller, Isr. J. Chem. 8 (1970) 259.
[31] D. Rehm, A. Weller, Z. Phys. Chem. 69 (1970) 183.
[32] V. Wintgens, J. Pouliquen, J. Kossanyi, M. Heintz, New J. Chem. 10 (1986) 345.
[33] Y. Kuriyama, T. Arai, H. Sakuragi, K. Tokumaru, Chem. Lett. (1988) 1193.
[34] R.A. Marcus, Annu. Rev. Phys. Chem. 15 (1964) 155.
[35] T. Sakurai, T. Obana, T. Inagaki, H. Inoue, J. Chem. Soc., Perkin Trans. II (1989) 535.
[36] R. Searle, J.L.R. Williams, D.E. DeMeyer, J.C. Doty, J. Chem. Soc., Chem. Commun. (1967) 1165.
[37] T. Sakurai, H. Sukegawa, H. Inoue, Bull. Chem. Soc. Jpn. 58 (1985) 2875, and references cited therein.
[38] C.G. Hatchard, C.A. Parker, Proc. R. Soc. London Ser. A 235 (1956) 518.
[39] L.W. Jones, C.N. Sneed, J. Am. Chem. Soc. 39 (1917) 674.
[40] J.A. Riddick, W.B. Bunger, T.K. Sakano, Organic Solvents, Wiley, Chichester, UK, 1986.
[41] H.E. Zimmerman, A.M. Weber, J. Am. Chem. Soc. 111 (1989) 995.